ELSEVIER

Contents lists available at ScienceDirect

Atmospheric Research

journal homepage: www.elsevier.com/locate/atmosres





An observational analysis of precipitation and deforestation age in the Brazilian Legal Amazon

Ye Mu^{a,*}, Charles Jones a,b

- ^a Department of Geography, University of California Santa Barbara, Santa Barbara, CA, USA
- ^b Earth Research Institute, University of California Santa Barbara, Santa Barbara, CA, USA

ARTICLE INFO

Keywords: Amazon Forest Rainfall variability Land-atmosphere interactions Deforestation Rain gauge

ABSTRACT

Rainfall in the Amazon is influenced by atmospheric circulation dynamics on multiple spatiotemporal scales. Anthropogenic influences such as deforestation, land-use changes, and global climate change are also critical factors in determining rainfall in South America. Modeling studies have projected a drier climate with the ongoing deforestation in the Amazon, but observational evaluation of the variability of rainfall and deforestation patterns has been limited. This study analyzes spatiotemporal trends in rainfall between 1981 and 2020 and relationships with deforestation age in the Brazilian Legal Amazon (BLA). An improved rainfall dataset is derived by calibrating the Climate Hazards Group Infrared Precipitation with Stations (CHIRPS) data with observations from a rain gauge network in the BLA. Trend analysis is employed to identify significant changes in precipitation over the BLA. Satellite-based land cover data Mapbiomas and ET datasets are used to evaluate similar trends. While large spatial variability is observed, the results show coherent relationships between negative dry-season rainfall trends and old-age deforested areas. Deforestation aged up to a decade enhanced rainfall and older deforested regions have reduced rainfall during the dry season. These results suggest substantial changes in the hydroclimate of the BLA and increased vulnerability to future land cover change.

1. Introduction

The Amazon forest plays vital roles in climate patterns, ecosystems, hydrological cycling, carbon storage, and biodiversity. Rainfall information for the Amazon is important for economic services, water resources, and climate variability applications (Cavalcante et al., 2020). The Amazon exhibits high spatiotemporal variability of rainfall. The ongoing deforestation in the Brazilian Legal Amazon (BLA) can trigger substantial feedbacks with surface temperatures, evapotranspiration (ET), and rainfall from local-to-continental scales.

The Amazon, on average, experiences extreme flood or drought events every 10 years, and the decadal variations in the intensity and frequency of extreme events can have significant environmental and socioeconomic consequences in the region (Marengo et al., 2011; Zilli et al., 2017; Cerón et al., 2022). Extreme events are associated with local, regional and global atmospheric circulation patterns. In South America, rainfall variability is affected by the South Atlantic Convergence Zone (SACZ), Intertropical Convergence Zone (ITCZ), Bolivian High (BH), Costal Squall Lines (CSL), and local-scale systems (De Souza and Ambrizzi, 2004; Santos et al., 2015). Yet, climate variability is also

Human-caused environmental disturbances in South America have been historically large. Roughly, 20% of the forest cover in the BLA has been converted to pasture, agricultural lands and other land uses (Souza Jr et al., 2013). Deforestation is linked to changes in the amount and distribution of rainfall at a variety of spatial and temporal scales, therefore influencing local and regional climates (Davidson et al., 2012; Lawrence and Vandecar, 2014; Mu et al., 2021a). Durieux (2003)'s analysis of cloud cover and precipitation trends suggested that a regional climate change may already be underway in the most deforested part of the arc of deforestation, and the deforestation may lead to increased seasonality. Thus, it is important to further understand the spatiotemporal variability of rainfall in the BLA, identify and quantify potential linkages with land-cover land-use changes (Haghtalab et al., 2020).

E-mail address: ye.mu@geog.ucsb.edu (Y. Mu).

associated with large-scale tropical circulation mechanisms, including the El Niño/Southern Oscillation (ENSO) and the Pacific Decadal Oscillation (PDO) (Marengo and Espinoza, 2016). Intraseasonal and submonthly climate variability is also influenced by the interhemispheric sea surface temperature (SST) gradients in the Atlantic Ocean (De Souza et al., 2005; Cerón et al., 2021).

^{*} Corresponding author.

The ability to understand changes in rainfall patterns from in-situ measurements is limited due to the sparse rain gauge network (Silva Junior et al., 2018). Thus, rainfall data estimated from remote sensing or reanalyses are viable options for detecting changes in rainfall. The Climate Hazards Group InfraRed Precipitation with Station data (CHIRPS) provides blended gauge-satellite precipitation with 0.05° latitude/longitude grid spacing and daily to annual temporal resolutions spanning 50°S-50°N from 1981 to the present and it can be used for trend analysis and seasonal drought monitoring (Funk et al., 2015). CHIRPS has been validated in different regions of the globe (Hessels, 2015; Katsanos et al., 2016; Bai et al., 2018; Wu et al., 2019; Cavalcante et al., 2020; Nawaz et al., 2021). CHIRPS shows good performance in different studies. For the Brazil Amazon, CHIRPS has been validated against 45 rain gauges, showing an underestimation of extreme rainfall indices (Cavalcante et al., 2020). Paca et al. (2020) validated CHIRPS with 98 gauges in the Amazon basin and Paredes-Trejo et al. (2017) used 21 gauges in Northeast Brazil.

Satellite-only rainfall estimates have significant uncertainty because none of the satellite sensors directly measure rainfall (Tian and Peters-Lidard, 2010). In contrast, previous observational studies based on rain gauges-only are unable to accurately characterize spatial variations in trends over the Amazon (Angelis et al., 2004; Almeida et al., 2017). Almeida et al. (2017) found that future studies with more weather stations and longer periods would improve the spatial analysis of rainfall trends and could increase the understating of rainfall variability. These conclusions motivate the development of additional datasets blending satellite data with rain gauges rainfall to improve trend analysis (Cavalcante et al., 2020; Mu et al., 2021b).

This study aims to contribute to this research effort to determine trends in rainfall and linkages with land-use land-cover changes over the BLA. Specifically, the objectives of this study are: (a) to develop an improved dataset Brazilian Amazon CHIRPS (baCHIRPS) from 1981 to 2020 by blending CHIRPS with a rain gauge network in the BLA; (b) to examine the relationships between the age of deforestation and dryseason rainfall in the BLA. The main strength of the study is that it uses a large number of rain gauges observations for validation and blending over a 40-year period, and it examines the dry season rainfall in relation to the age of deforestation and ET. Section 2 describes the study region, data, and analysis methods. The results are presented and discussed in Section 3. The summary and conclusions are in Section 4.

2. Materials and methods

2.1. Study area

The study area covers the BLA, an area of 5 million km² including the states of Acre, Amapá, Amazonas, Mato Grosso, Pará, Rondônia, Roraima, Tocantins, and part of Maranhão State located west of 44°W longitude (Fig. 1). The Amazon region is characterized by having a moist atmosphere with average annual rainfall between 1400 mm and 3000 mm (Cavalcante et al., 2020). The climate varies over the BLA, and it is influenced by various physical and dynamical processes on local, regional and large scales (Santos et al., 2015). The northwest part of the region features a continuous rainy season, but wet/dry transitional and long dry season climate in the south and east (Davidson et al., 2012). Within the BLA, the Arc of Deforestation is located in the southeastern region, where the forest has been converted to agriculture and pasture lands since 1970 (INPE, 2020).

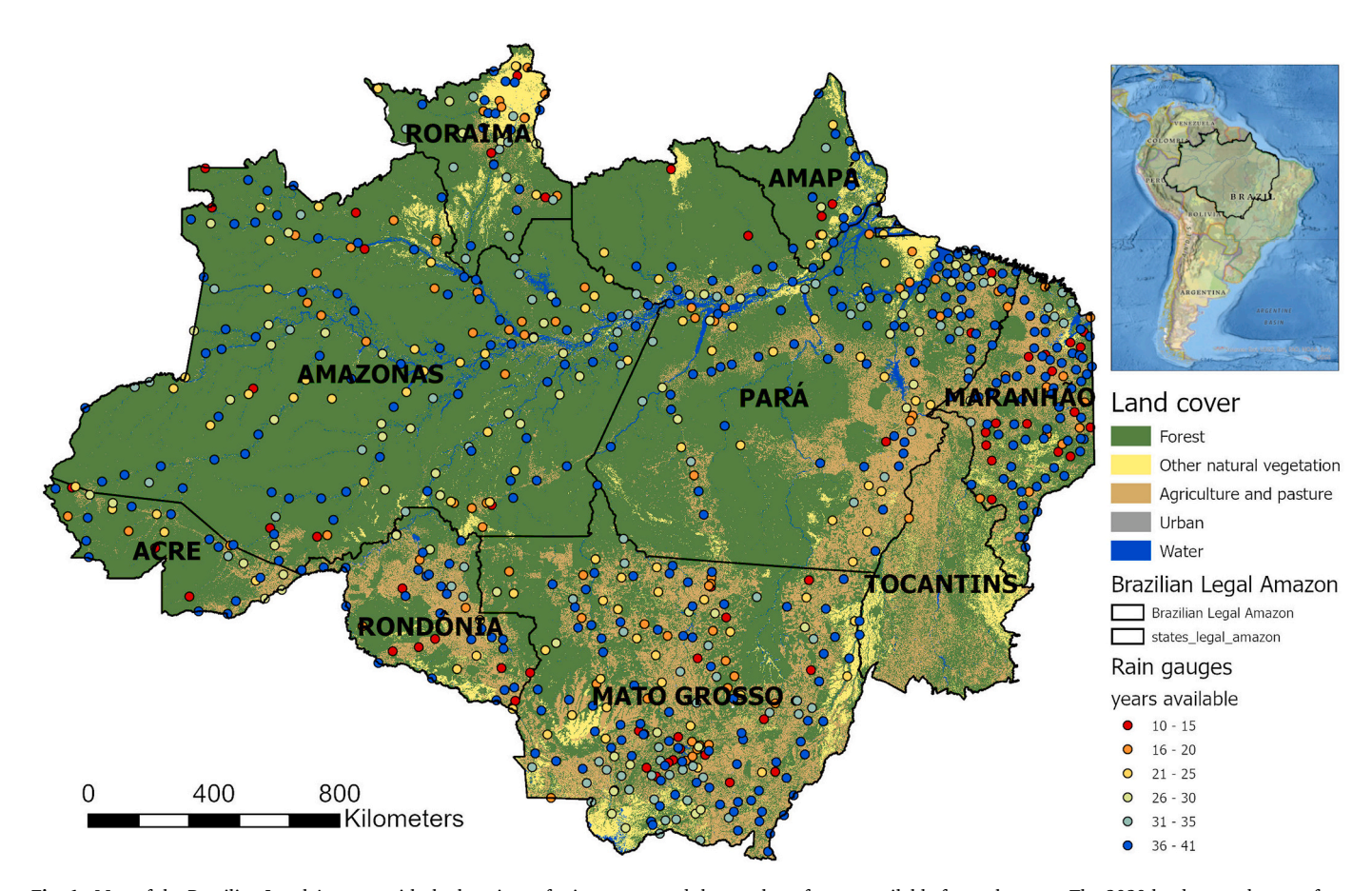


Fig. 1. Map of the Brazilian Legal Amazon with the locations of rain gauges, and the number of years available for each gauge. The 2020 land cover data are from Mapbiomas Project Collection 6 (Mapbiomas Project, 2021).

2.2. Rainfall data

Daily rainfall data were obtained from the Brazilian National Water Agency (ANA) (available at http://www.snirh.gov.br/hidroweb/). For the BLA, a total of 1034 rain gauges were acquired from 1981 to 2020. For this analysis, inventory and quality control of the rain gauge data was conducted in two steps: (a) calculate monthly rainfall from daily values and examine data availability as a percentage of days for each month and year. (b) months that have quality flags of blank, uncertain, and estimated for any day were removed; (c) exclude gauges with records shorter than 10 years after 1981. This resulted in 765 gauges over the study area.

The satellite-based rainfall product CHIRPS from the Climate Hazard Group was used for this analysis (available online at https://data.chc. ucsb.edu/products/CHIRPS-2.0/). According to Funk et al. (2014), CHIRPS includes several data sources: (1) monthly (six pentads per month) precipitation climatology CHPClim; (2) quasi-global geostationary thermal infrared (IR) satellite observations from the NOAA data. products of the Climate Prediction Center (CPC) and the B1 IR from the National Climatic Data Center; and (3) in-situ precipitation from a variety of sources such as the Global Historical Climate Network (GHCN), the Global Summary of the Day dataset (GSOD) and the World Meteorological Organization's Global Telecommunication System daily data provided by NOAA CPC and over a dozen of public and private meteorological services. Monthly CHIRPS data were used from January 1981 to December 2020 at a spatial resolution of 0.05° (about 5.3 km over the Amazon region) (Funk et al., 2014), which overlaps with the ANA rain gauges data period.

2.3. Deforestation and ET data

The deforestation age is the year a pixel transitioned from forested to pasture and other non-vegetated land cover types. We calculated the age of deforestation in Google Earth Engine (GEE) using classified land cover data from Mapbiomas (2021) at 30-m resolution from 1985 to 2020. A full description of the Mapbiomas data is in Souza Jr. et al. (2020). We used ERA5-Land monthly reanalysis for ET trends analysis, which combines model data with observations from across the world (Hersbach et al., 2020). ERA5 ET also accounts for seasonally varying monthly vegetation maps from MODIS-based satellite datasets (Boussetta et al., 2013). The Global Land Evaporation Amsterdam Model (GLEAM) ET dataset was also used for comparison with ERA5 ET (Martens et al., 2017).

2.4. Data blending method

Here, a new rainfall dataset baCHIRPS (0.05° × 0.05° resolution, 1981–2020), was developed by blending the 765 calibration rain gauges data with CHIRPS using the Background-Assisted Station Interpolation for Improved Climate Surfaces (BASIICS) algorithm in Geospatial Climate Data Management and Analysis (GeoCLIM) software. GeoCLIM is developed and maintained by the United States Geological Survey (USGS) and Family Early Warning Systems Network (FEWS NET) (Pedreros and Tamuka, 2020). The BASIICS algorithm combines rain gauges with raster or gridded data to produce a more accurate gridded dataset using a modified Inverse Distance Weighting (IDW) that borrows some concepts from simple and ordinary kriging (Pedreros and Tamuka, 2020). We used modified IDW interpolation with the following parameters: 2.0 weight power, 500 km search radius and maximum effective distance, 0 (min) to 10 (max) gauges, 3.0 maximum ratio of the gauge to CHIRPS value, and a 1.0 fuzz factor. Following the method described in Funk et al. (2015), the blending process involved the following steps: a) Extract monthly grid values for all locations where the gauge data have valid values. This step produces a comparable gridded dataset that can be directly compared to the gauge values; b) ratios are calculated between the gauge and gridded values and these ratios are interpolated

using a modified IDW method; and c) the pixels are multiplied by the interpolated ratio layer if they are within the maximum effective distance, otherwise the original grid layer is used. The resulting monthly product is available from 1981 to 2020 and has the same spatial resolution as CHIRPS (0.05°).

2.5. Cross-validation

The resultant baCHIRPS data were cross-validated in the BASIICS blending process. For each gauge point, the validation produces a cross-validated value which is the blended grid value at the gauge location when the gauge is not included in the BASIICS (Cross-Validated baCHIRPS value), and the interpolated gauge value without blending in the background grid. We carried out point-to-pixel comparison statistics for these values. The root-mean-square error (RMSE) Eq. (1) and the coefficient of determination (R^2) Eq. (2) were used for statistical metrics.

$$RMSE = \sqrt{\frac{\sum_{i=1}^{n} (\text{grids} - \text{gauges})^{2}}{n}}$$
 (1)

$$R^{2} = \frac{\sum_{i=1}^{n} (\text{gauges}_{i} - \mu)^{2}}{\sum_{i=1}^{n} (\text{grids}_{i} - \mu)^{2}}$$
(2)

2.6. Rainfall data analysis and trends

The new blended rainfall data baCHIRPS was used for rainfall analysis. The average analysis method calculates the temporal average value for each pixel for a period. To investigate the difference anomaly for the average monthly rainfall for the baseline (1981–2020), the standardized anomaly method was used (Eq. (3)). The standardized anomaly expresses the difference anomaly as a percent of the standard deviation (SD).

$$stdanom = \frac{(average_{month} - average_{baseline}) + 0.1}{SD_{baseline} + 0.1}$$
(3)

Pixel-by-pixel trend analysis allowed us to identify a change in the expected rainfall value and the spatial distribution that occurred over a period of time. We used one non-parametric method to identify the magnitudes of trends in the study area. We calculated the monotonic trend based on the Kendall Tau statistic and the Theil-Sen slope (Sen, 1968; Kendall, 1975; Gilbert, 1987; Siegel, 1982; Theil, 1992) for the baCHIRPS gridded data time series. The Kendall Tau is a ratio of the actual correlation rating score to the maximum possible score. The dataset is sorted in ascending order by time to generate the rating score for a time series. The test statistic Tau results in a range between -1 to +1, with negative values indicating a downward trend (more negative "steps") and positive values indicating an upward trend (more upward "steps). To find significant trends, we utilized a significance threshold $\alpha = 0.05$. For more details on how both statistical tests are structured, see ElNesr et al. (2010).

3. Results and discussion

3.1. Cross-validation results

Fig. 2 shows rain gauge observations (N=765), and CHIRPS rainfall estimates at a monthly scale for the 1981–2020 period. Overall, CHIRPS shows a moderate estimation of the observed rainfall with an $\rm R^2$ of 0.74 and RMSE of 75.6 mm/month. There is an overestimation of the low rainfall values and an underestimation of high rainfall values. This suggests that rainfall estimation errors could occur for regions with extreme rainfall events. The number of gauges used in the CHIRPS data in Brazil is highly variable and decreased starting in 1985 and fell to a

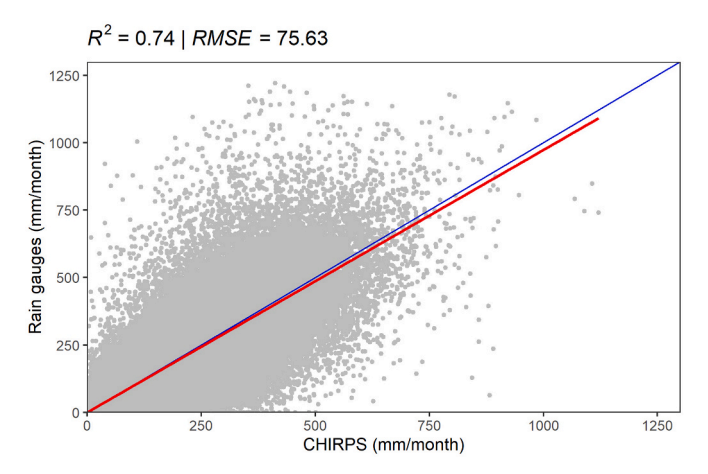


Fig. 2. CHIRPS-based rainfall estimates and rain gauges (N=765) and for the 1981–2020 period. Blue line indicates 1:1 correspondence and red line gives the linear regression best fit. (For interpretation of the references to colour in this figure legend, the reader is referred to the web version of this article.)

few hundreds by 2013 (Carvalho, 2020). Thus, the initial validation helps to determine that the CHIRPS dataset is correlated with rain gauges, but a blended satellite-gauge dataset can provide improved results. (Pedreros and Tamuka, 2020). Fig. 3 shows the at-gauge interpolated gauge values without satellite background against CHIRPS values and cross-validated baCHIRPS values. Note that both the interpolated gauges and cross-validated baCHIRPS values exclude that gauge used for blending. The cross-validation result shows that baCHIRPS ($R^2 = 0.95$, RMSE = 29.2 mm/month) better represent the values of rain gauges than the original CHIRPS ($R^2 = 0.88$, RMSE = 44.6 mm/month). baCHIRPS, blended with rain gauges, has higher accuracy in estimating

high and low rainfall values (Fig. 3). The baCHIRPS is therefore, used in the following trend and spatial analyses over the BLA.

3.2. Monthly rainfall anomalies

To examine how much wetter and drier the BLA was for a month, we calculated the difference anomaly for the average monthly precipitation for each year and expressed it in terms of standard deviations away from the mean. Fig. 4 shows the standardized anomalies of monthly mean rainfall for the BLA from 1981 to 2020. Extreme positive values are identified in 1989 (1.11 in June, 0.79 in July, and 0.91 in August), 1984 (1.16 in September), 1994 (1.34 in June), and 2009 (0.82 in May and 1.04 in June). The extreme positive anomalies in 1989 and 2009 were associated with extreme seasonal flood events. Floods in the Amazon in 1989 were related to La Niña that impacted rainfall (Marengo et al., 2012; Espinoza et al., 2013). In the year 2009, the flood event was related to an anomalously southward migration of ITCZ during May–June 2009 due to the warming in the Tropical South Atlantic (TSA) (Marengo et al., 2010; Marengo et al., 2012).

Low negative values are observed in 1983 (-0.86 in January and -0.76 in May), 1995 (-0.75 in August), 1997 (-0.82 in July, -0.73 in October), 1998 (-0.66 in February), 2005 (-0.5 from June to August), 2010 (-0.74 in September and -0.61 in March), 2015 (-1.01 in September, -0.83 in October, -0.85 in November and -1.12 in December), and 2016 (-0.76 in February). Marengo and Espinoza (2016) reported that deficient rainfall in 1983, 1995, 1997–1998, 2005, and 2010 caused anomalously low river levels and increased fires in Amazonia. The negative rainfall anomalies are associated with extreme drought events that occurred in the Amazon in 1995, 1997–1998, 2005, 2010, and 2015–2016, which were related to the El Niño-Southern Oscillation (ENSO), warming of the Tropical North Atlantic (TNA) Ocean, or a combination of both (Lewis et al., 2011; Marengo et al.,

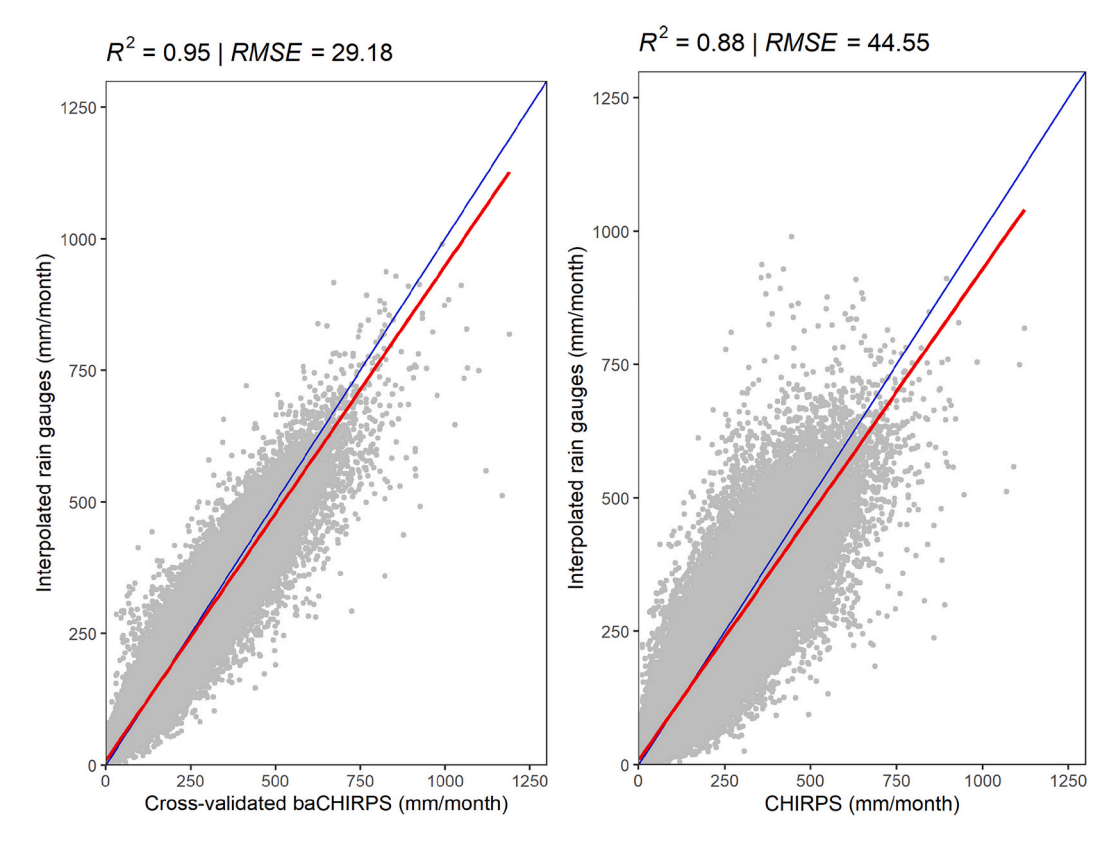


Fig. 3. Interpolated rain gauges and cross-validated baCHIRPS (left) and CHIRPS (right) for the 1981–2020 period (N = 249,067). The blue line indicates 1:1 correspondence and the red line gives the linear regression best fit. (For interpretation of the references to colour in this figure legend, the reader is referred to the web version of this article.)

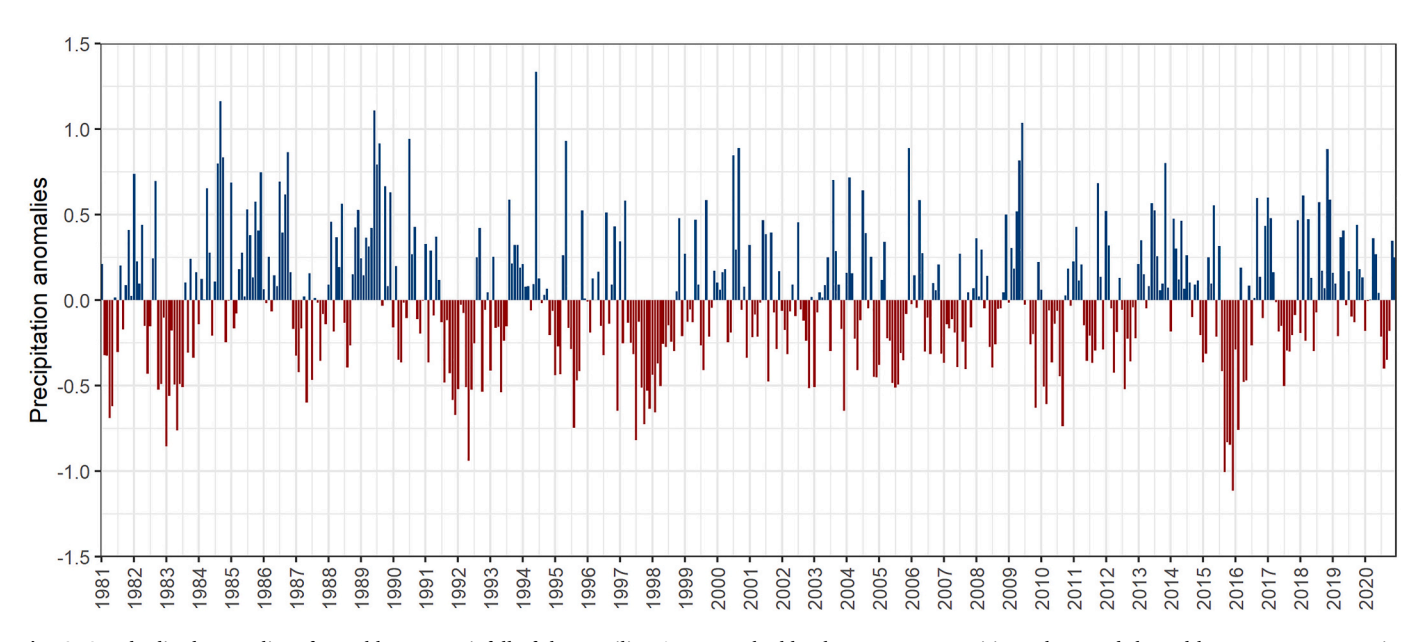


Fig. 4. Standardized anomalies of monthly mean rainfall of the Brazilian Amazon. The blue bars represent positive values, and the red bares represent negative anomalies. (For interpretation of the references to colour in this figure legend, the reader is referred to the web version of this article.)

2011; Jiménez-Muñoz et al., 2016). Our results show that 2015 had the highest rainfall deficit over the past 40 years in BLA, which is consistent with Panisset et al. (2018) who reported that this drought episode exceeded the amplitude and spatial extent of the previous events that affected more than 80% of the Amazon basin. The 2015 extreme drought event was driven by ENSO combined with the regional warming trend (Jiménez-Muñoz et al., 2016).

3.3. Spatiotemporal trends and variability

Fig. 5 shows the Tau statistics for the baCHIRPS data with hatched areas indicating statistically significant annual trends at the 0.05 level. The baCHIRPS data have rain gauges blended in, and shows improvement in rainfall trends identification, which is consistent with previous studies (Cavalcante et al., 2020; Mu et al., 2021b). The results show that significant positive and negative trends are present throughout the BLA. The northern and central parts of the domain show significant positive trends, while southern Roraima, central Amapá, northeastern and western Amazonas have large areas with Tau $>\!0.3$. Significant negative trends are mainly located over the states of Rondônia and Amazonas,

southern Mato Grosso, western Amazonas down to easter Acre, and northern Mato Grosso up to southern Pará.

Amazon rainfall varies on seasonal scales such that maximum rainfall occurs in December–February (DJF) over the central-western and southern Amazon and maximum in March–May (MAM) over the eastern and central Amazon (Angelis et al., 2004). South of the Equator, the dry season is more evident in June–August (JJA), while the equatorial northern part does not have a well-defined dry season (Ronchail et al., 2002). Here, we define the seasons as Summer DJF; Autumn MAM; Winter JJA; Spring SON, which had also been used in previous studies (Cavalcante et al., 2020; Regoto et al., 2021).

Fig. 6 shows the Kendall Tau values for the seasonal rainfall trends. In all seasons, the overlapping regions with significant trends are similar to the annual trends in Fig. 5. During DJF, positive rainfall trends are observed from the central to western BLA, while western Amazonas, southern Rondônia, and north and northwest parts of the Mato Grosso experience negative trends. During MAM, a positive rainfall trend is more evident from the northern to eastern BLA, especially in the states of Roraima, Amapa, and Tocantins. Based on baCHIRPS and previous studies (Silva Junior et al., 2018; Haghtalab et al., 2020), rainfall trends

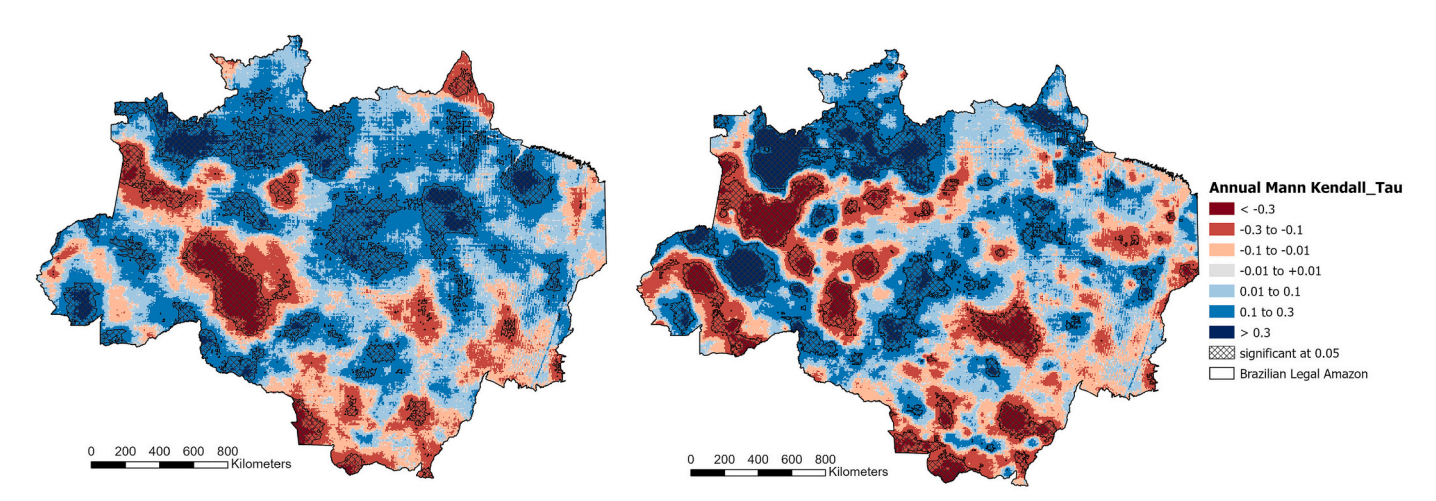


Fig. 5. Trends of mean annual precipitation of CHIRPS (left) and baCHIRPS (right) over the Brazilian Amazon in the period 1981–2020. Hatches show significant trends at a 5% confidence level.

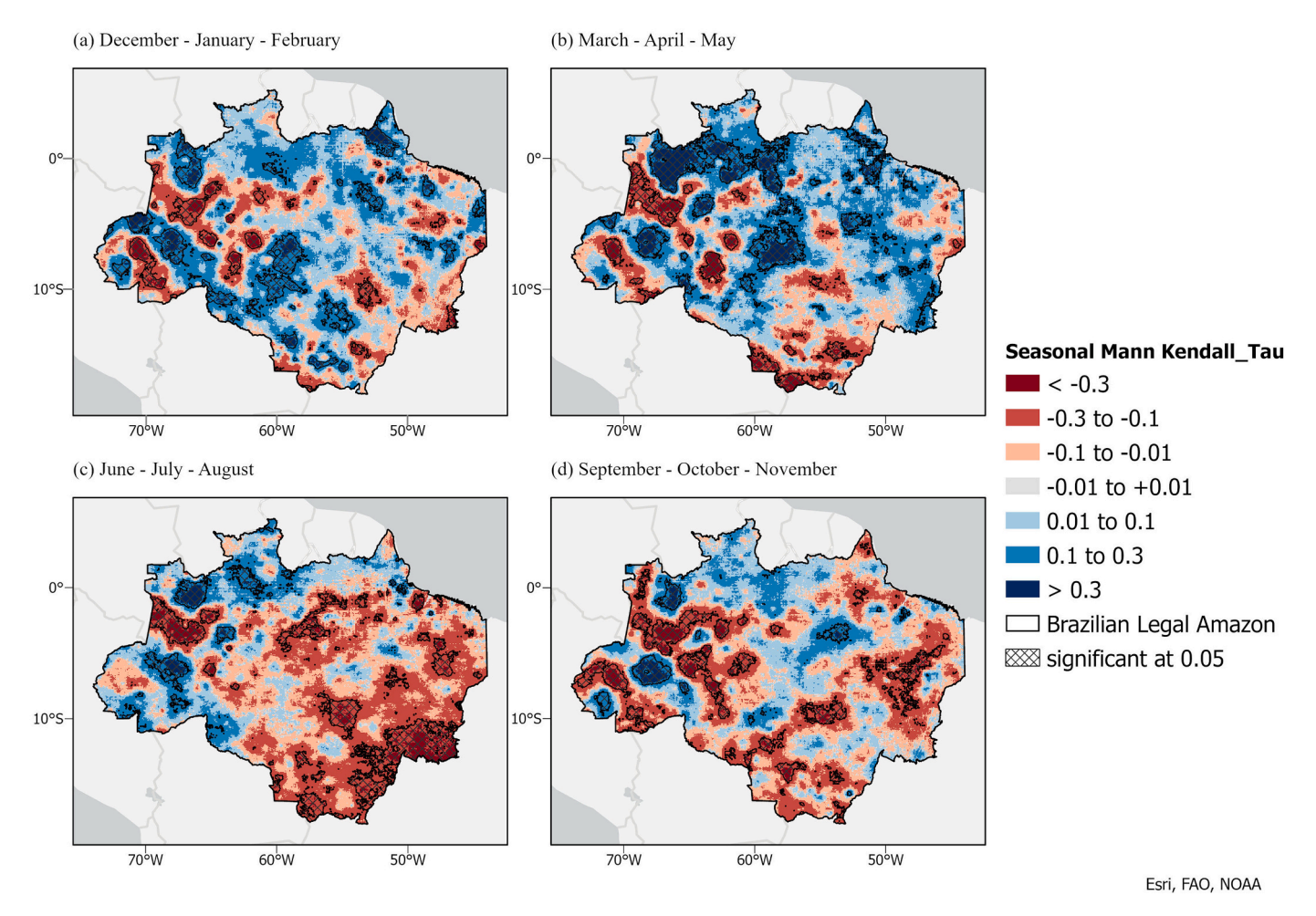


Fig. 6. Trends of mean seasonal precipitation for (a) DJF, (b) MAM, (c) JJA, and (d) SON estimated by baCHIRPS in the Brazilian Amazon.

during the wet season are spatially heterogeneous. During both DJF and MAM, negative trends tend to be collocated over the same regions (Fig. 6a and b). In the dry season, negative trends are found in the central, southern, and southeastern regions of the domain, which is consistent with other studies (Almeida et al., 2017; Silva Junior et al., 2018). Precipitation indices also showed increasing consecutive dry days over almost all of Brazil (Avila-Diaz et al., 2020b, 2020a). While the dry season rainfall variations are associated with ENSO and the warming of the TNA, large areas of significant negative trends (Tau < -0.3) are over the "arc of deforestation" in the southern and eastern parts of the basin (Fig. 6c and d).

3.4. Deforestation, ET, and rainfall

Other studies have found increased dry season length over the southern Amazon (Fu et al., 2013; Debortoli et al., 2015). The June–September (JJAS) dry season period is intensively used for deforestation, which coupled with economic and social activities contributes to the "arc of deforestation" regions (Khanna et al., 2017) (see also Fig. 1). To investigate possible linkages among the spatial extent of deforestation and trends in ET and rainfall, Fig. 7 shows deforested areas as of 2020 (Mapbiomas, 2021), JJAS ET and rainfall trends. Note that deforestation areas are mapped according to the age of deforestation. Focusing on the southern Amazon, heavily deforested regions show significant negative rainfall trends during the dry season. In Fig. 7a, it is important to highlight that regions with old ages of deforestation (dark brown areas) have more significant negative dry season rainfall trends. In Fig. 7a, the time series of JJAS ET and rainfall of three regions were

shown, including the agricultural belts in Rondônia (left), Mato Grosso (bottom), and eastern Pará (right). These three regions have been largely deforested since 1985, and negative dry-season rainfall trends are shown. However, the time series of JJAS ET from ERA5 and GLEAM did not have any consistent trends. To further validate the dry-season rainfall trends, baCHIRPS grids with more than 50% deforestation were identified across the BLA. Fig. 7b shows the age of deforestation for each over 50% deforested grid against its JJAS rainfall trends.

Regions with older ages of deforestation have longer years of forest conversion and, thus, larger percentages and sizes of deforested land. The large-scale and older deforested regions also show large negative trends in rainfall (Fig. 7a and b). Dry-season rainfall was enhanced at the 0-10 age groups, and reduction occurred after the 10-15 age of deforestation (Fig. 7b), suggesting a critical deforestation threshold for rainfall reduction. This dual deforestation impact on rainfall are consistent with other studies (Da Silva et al., 2008; Nobre et al., 2009; Leite-Filho et al., 2021). A shift from small-scale to large-scale deforestation in the southern Amazon is found to modify the mechanisms and patterns of regional rainfall (Chambers and Artaxo, 2017). Empirical and modeling studies showed that large-scale deforestation influences cloud cover and rainfall (Gash and Nobre, 1997; Durieux, 2003; Ray et al., 2006; Leite-Filho et al., 2021). Deforestation alters the hydrological and energy balances by reducing evapotranspiration, increasing sensible heat flux, and decreasing latent heat flux. Additionally, deforestation decreases surface roughness and increases surface albedo, which induces a decrease in absorbed solar radiation (Davidson et al., 2012). The Amazon rainfall is highly dependent on recycled moisture since up to 70% of rainfall in the southern basin originates from

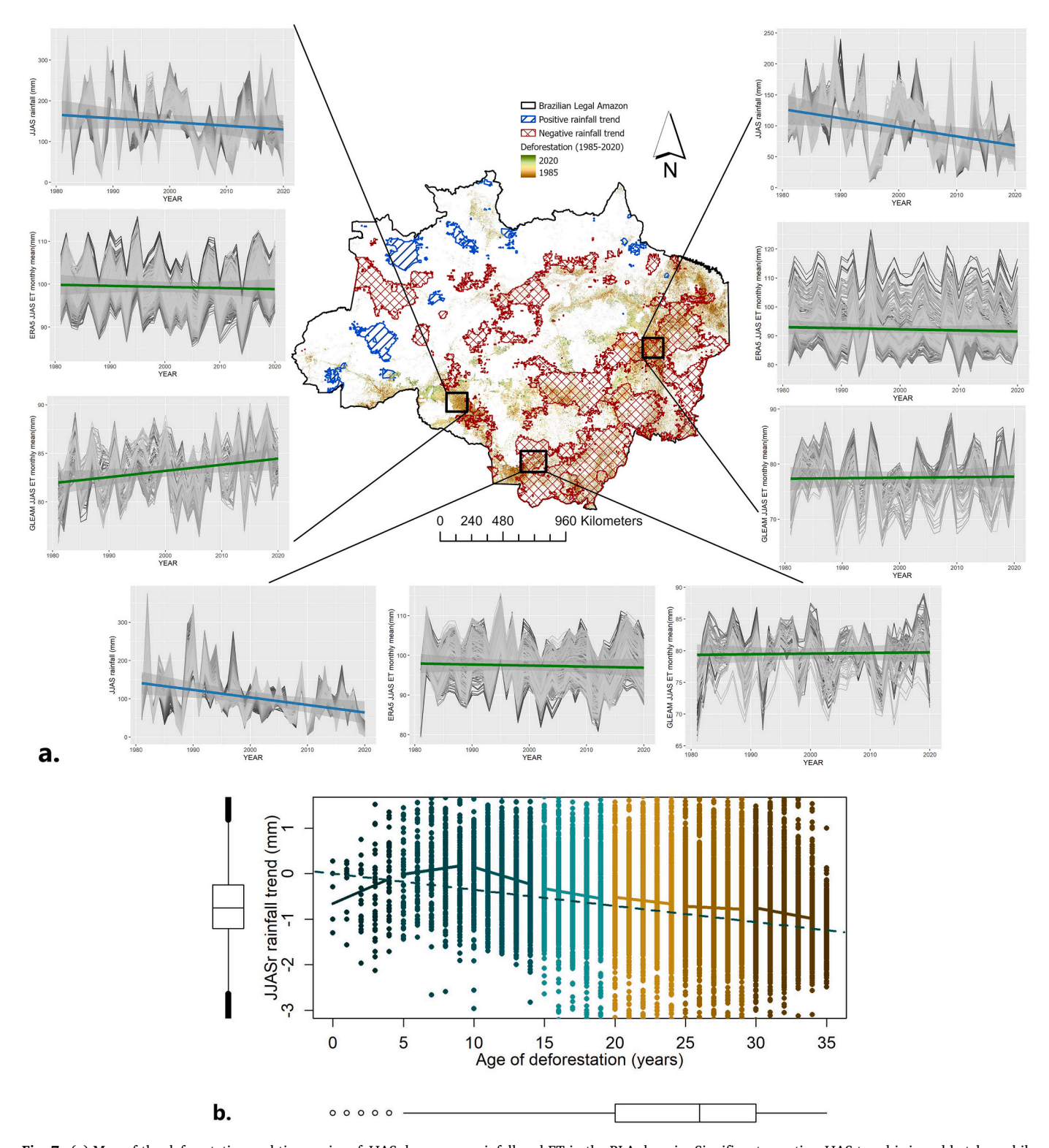


Fig. 7. (a) Map of the deforestation and time series of JJAS dry season rainfall and ET in the BLA domain. Significant negative JJAS trend is in red hatches while significant positive trends are in blue hatches. Gray curves are the time series of all grids in each region, and green/blue lines are the trends. (b) Scatterplot of the age of deforestation and JJAS rainfall trend in the BLA. The solid lines indicate the regression slope for each group at the 5 years interval. The dashed line indicates the overall trend line. (For interpretation of the references to colour in this figure legend, the reader is referred to the web version of this article.)

terrestrial ET upwind (van der Ent et al., 2010; Staal et al., 2018). Furthermore, the dry season may be more significantly affected by deforestation because it is typically driven by locally generated convection, shifting from a thermally to a dynamically driven hydroclimatic regime (Malhi et al., 2008; Khanna et al., 2017). The results of sensitivity analysis on the ET trends over the old-frontier deforested regions show

that different ET datasets have high variability and uncertainty in the study regions. ET can be estimated from point observations, remote sensing products, and process modeling at various spatiotemporal resolutions, and it is a poorly measured variable in the Amazon (Sörensson and Ruscica, 2018; Builes-Jaramillo and Pántano, 2021). ET estimates from land surface models and remote sensing have uncertainties, and

South America is very poorly covered with flux towers (Long et al., 2014; Sörensson and Ruscica, 2018). Thus, further study is needed on the ET estimates in the region to improve our understanding of the regional climate interactions.

4. Summary and conclusions

We analyzed spatial and temporal rainfall patterns and trends using improved satellite-based rainfall estimates calibrated with rain gauges over the Brazilian Legal Amazon during 1981-2020. We have examined the impacts of deforestation on dry-season rainfall in the Brazilian Legal Amazon. Despite the limitations of available in-situ rain gauges in the Brazilian Amazon, we developed an improved blended satellite-rain gauges rainfall dataset over a 40-year period to understand changes in rainfall. Our results show that the northwest region continues to have a rainy climate, a wet/dry transitional climate in the center, and a long dry season climate in the south and east. However, the rainfall trends are very heterogeneous without a characteristic pattern over the entire region. The trend in rainfall generally means that the wet season gets wetter and/or the dry season gets drier, but the significant localized trends show that it is more complex over the entire region (Haylock et al., 2006; Haghtalab et al., 2020; Regoto et al., 2021). In the southern region, large areas with significant dry season rainfall trends are located along the "arc of deforestation". Deforestation aged up to a decade enhanced dry-season rainfall and older deforested regions have reduced rainfall during the dry season. Widespread old-frontier deforested regions could alter the local hydroclimatic balances (Wongchuig et al., 2021). Leite-Filho et al. (2021) found that rainfall in the southern Brazilian Amazon decreases if deforestation exceeds a threshold, and this threshold is lower at large scales with rainfall reducing precipitously. Future projections also show that deforestation is estimated to reduce rainfall greater than natural variability by 2050 (Garcia-Carreras and Parker, 2011). Although the negative rainfall trends are not purely due to land-use changes (Parsons, 2020), the drought-deforestation feedback can be strengthened with cumulative deforestation (Staal et al., 2020; Mu et al., 2021a).

Although this study does not investigate causality, the results presented improved high-resolution rainfall estimates and can support additional studies to investigate drivers of rainfall changes in the Brazilian Amazon. Future studies can expand the study region to the entire Amazon Basin and examine how the patterns in the rainfall trends in the Amazon are related to climate variabilities, interhemispheric SST gradient in the Atlantic, and land-use change in the region. Further studies can also investigate the inconsistent trends among ET datasets to improve our understanding of the deforestation impacts on ET and land-atmosphere interactions in the Amazon. Some studies argue that the Amazon is projected to experience a drier climate than in the present and be exposed to more extreme events (Malhi et al., 2008; Davidson et al., 2012; Parsons, 2020). Extreme drought events can become more common through higher frequency and severity of ENSO events, rainfall reduction due to deforestation, forest fires, and climate change.

Acknowledgments, samples, and data

CHIRPS data were obtained from https://www.chc.ucsb.edu/data/chirps. The gauge data were obtained from https://www.snirh.gov.br/hidroweb/apresentacao. Mapbiomas land cover data were downloaded from mapbiomas.org and ERA5 are freely available at https://cds.climate.copernicus.eu/cdsapp. GLEAM ET data are available from https://www.gleam.eu/#1. We acknowledge Pete Peterson from the Climate Hazards Center for providing feedback and helpful discussion. C. Jones would like to thank the financial support from NSF (AGS 1937899).

CRediT authorship contribution statement

Ye. Mu: Conceptualization, Data curation, Formal analysis, Investigation, Methodology, Resources, Software, Validation, Visualization, Writing – original draft, Writing – review & editing. **Charles Jones:** Conceptualization, Methodology, Validation, Resources, Supervision, Writing – review & editing.

Declaration of Competing Interest

The authors declare that they have no known competing financial interests or personal relationships that could have appeared to influence the work reported in this paper.

References

- Almeida, C.T., Oliveira-Júnior, J.F., Delgado, R.C., Cubo, P., Ramos, M.C., 2017. Spatiotemporal rainfall and temperature trends throughout the Brazilian Legal Amazon, 1973-2013. Int. J. Climatol. 37 (4), 2013–2026. https://doi.org/10.1002/joc.4831.
- Angelis, C.F., Mc Gregor, G.R., Kidd, C., 2004. Diurnal cycle of rainfall over the Brazilian Amazon. V Ol. 26, 139–149.
- Avila-Diaz, A., Abrahão, G., Justino, F., Torres, R., Wilson, A., 2020a. Extreme climate indices in Brazil: evaluation of downscaled earth system models at high horizontal resolution. Clim. Dyn. 54, 5065–5088. https://doi.org/10.1007/s00382-020-05272-0
- Avila-Diaz, A., Benezoli, V., Justino, F., Torres, R., Wilson, A., 2020b. Assessing current and future trends of climate extremes across Brazil based on reanalyses and earth system model projections. Clim. Dyn. 55, 1403–1426. https://doi.org/10.1007/ s00382-020-05333-z.
- Bai, L., Shi, C., Li, L., Yang, Y., Wu, J., 2018. Accuracy of CHIRPS satellite-rainfall products over mainland China. Remote Sens. 10, 362. https://doi.org/10.3390/rs10030362
- Boussetta, S., Balsamo, G., Beljaars, A., Kral, T., Jarlan, L., 2013. Impact of a satellite-derived leaf area index monthly climatology in a global numerical weather prediction model. Int. J. Remote Sens. 34 (9–10), 3520–3542.
- Builes-Jaramillo, A., Pántano, V., 2021. Comparison of spatial and temporal performance of two Regional Climate Models in the Amazon and La Plata river basins. Atmos. Res. 250, 105413.
- Carvalho, L.M.V., 2020. Assessing precipitation trends in the Americas with historical data: a review. WIRES Clim. Chang. 11, e627 https://doi.org/10.1002/wcc.627.
- Cavalcante, R., Ferreira, D., Pontes, P., Tedeschi, R., Wanzeler da Costa, C., De Souza, E., 2020. Evaluation of extreme rainfall indices from CHIRPS precipitation estimates over the Brazilian Amazonia. Atmos. Res. 238, 104879. https://doi.org/10.1016/j. atmosres.2020.104879.
- Cerón, W.L., Kayano, M.T., Andreoli, R.V., Avila-Diaz, A., Ayes, I., Freitas, E.D., Martins, J.A., Souza, R.A.F., 2021. Recent intensification of extreme precipitation events in the La Plata Basin in Southern South America (1981-2018). Atmos. Res. 249, 105299 https://doi.org/10.1016/j.atmosres.2020.105299.
- Cerón, W.L., Andreoli, R.V., Kayano, M.T., Canchala, T., Ocampo-marulanda, C., Aviladiaz, A., Antunes, J., 2022. Trend pattern of heavy and intense rainfall events in Colombia from 1981–2018: a trend-EOF approach. Atmosphere (Basel) 13, 156. https://doi.org/10.3390/atmos13020156.
- Chambers, J.Q., Artaxo, P., 2017. Deforestation size influences rainfall. Nat. Clim. Chang. 7 (3), 175–176. https://doi.org/10.1038/nclimate3238.
- Da Silva, R.R., Werth, D., Avissar, R., 2008. Regional impacts of future land-cover changes on the Amazon basin wet-season climate. J. Clim. 21, 1153–1170. https:// doi.org/10.1175/2007JCLI1304.1.
- Davidson, E.A., de Araujo, A.C., Artaxo, P., Balch, J.K., Brown, I.F., Wofsy, S.C., 2012. The Amazon basin in transition. Nature 481 (7381), 321–328. https://doi.org/ 10.1038/nature10717.
- De Souza, E.B., Ambrizzi, T., 2004. Pentad precipitation climatology over Brazil and the associated atmospheric mechanisms. Climan'alise 2 (1), 1–20.
- De Souza, E., Kayano, M., Ambrizzi, T., 2005. Intraseasonal and submonthly variability over the Eastern Amazon and Northeast Brazil during the autumn rainy season. Theor. Appl. Climatol. 81, 177–191. https://doi.org/10.1007/s00704-004-0081-4.
- Debortoli, N.S., Dubreuil, V., Funatsu, B., Delahaye, F., Oliveira, C., Rodrigues-Filho, S., Saito, C., Fetter, R., 2015. Rainfall patterns in theSouthern Amazon: a chronological perspective (1971–2010). Clim. Chang. 132 (2), 251–264. https://doi.org/10.1007/s10584-015-1415-1.
- Durieux, L., 2003. The impact of deforestation on cloud cover over the Amazon arc of deforestation. Remote Sens. Environ. 86 (1), 132–140. https://doi.org/10.1016/ s0034-4257(03)00095-6.
- ElNesr, M.N., Abu-Zreig, M.M., Alazba, A.A., ElNesr, M.N., Abu-Zreig, M.M., Alazba, A. A., 2010. Temperature trends and distribution in the Arabian peninsula. Am. J. Environ. Sci. 6 (2), 191–203. https://doi.org/10.3844/ajessp.2010.191.203.
- Espinoza, J.C., Ronchai, L.J., Frappart, F., Lavado, W., Santini, W., Guyot, J.L., 2013. The major floods in the Amazonas river and tributaries (Western Amazon basin) during the 1970–2012 period: a focus on the 2012 flood. J. Hydrometeorol. 14 (3), 1000–1008. https://doi.org/10.1175/JHM-D-12-0100.1.

- Fu, R., Yin, L., Li, W., Arias, P.A., Dickinson, R.E., Huang, L., Chakraborty, S., Fernandes, K., Liebmann, B., Fisher, R., Myneni, R.B., 2013. Increaseddry-season length over southern Amazonia in recent decades and itsimplication for future climate projection. Proc. Natl. Acad. Sci. U. S. A. 110 (45), 18110–18115. https:// doi.org/10.1073/pnas.1302584110.
- Funk, C.C., Peterson, P.J., Landsfeld, M.F., Pedreros, D.H., Verdin, J.P., Rowland, J.D., Romero, B.E., Husak, G.J., Michaelsen, J.C., Verdin, A.P., 2014. A quasi-global precipitation time series for drought monitoring. U.S. Geol. Surv. Data Ser. 832, 4. https://doi.org/10.3133/ds832.
- Funk, C., Peterson, P., Landsfeld, M., Pedreros, D., Verdin, J., Shukla, S., Husak, G., Rowland, J., Harrison, L., Hoell, A., Michaelsen, J., 2015. The climate hazards infrared precipitation with stations—a new environmental record for monitoring extremes. Sci. Data 2, 150066. https://doi.org/10.1038/sdata.2015.66.
- Garcia-Carreras, L., Parker, D.J., 2011. How does local tropical deforestation affect rainfall? Geophys. Res. Lett. 38 (19) https://doi.org/10.1029/2011gl049099.
- Gash, J.H.C., Nobre, C.A., 1997. Climatic effects of Amazonian defor-estation: some results from ABRACOS. Bull. Am. Meteorol. Soc. 78, 823–830. https://doi.org/ 10.1175/1520-0477(1997)078<0823:CEOADS>2.0.CO;2.
- Gilbert, R.O., 1987. Statistical Methods for Environmental Pollution Monitoring. Van Nostrand Reinhold, New York, p. 336. ISBN: 978-0-471-28878-7.
- Haghtalab, N., Moore, N., Heerspink, B.P., et al., 2020. Evaluating spatial patterns in precipitation trends across the Amazon basin driven by land cover and global scale forcings. Theor. Appl. Climatol. 140, 411–427. https://doi.org/10.1007/s00704-019-03085-3
- Haylock, M., Peterson, T.C., Alves, L.M., Ambrizzi, T., Anunciação, M.T., Baez, J., Barros, V.R., Berlato, M.A., Bidegain, M., Coronel, G., Corradi, V., Garcia, V.J., Grimm, A.M., Karoly, D., Marengo, J.A., Marino, M.B., Moncunill, D.F., Nechet, D., Quintana, J., Rebello, E., Rusticucci, M., Santos, J.L., Trebejo, I., Vicent, L.A., 2006. Trends in Total and Extreme South American Rainfall in 1960-2000 and Links with Sea Surface Temperature. J. Clim. 19, 1490–1512. https://doi.org/10.1175/JCLISCS.1
- Hersbach, H., Bell, B., Berrisford, P., et al., 2020. The ERA5 global reanalysis. Q. J. R. Meteorol. Soc. 146, 1999–2049. https://doi.org/10.1002/qj.3803.
- Hessels, T.M., 2015. Comparison and Validation of Several Open Access Remotely Sensed Rainfall Products for the Nile Basin. Delft University of Technology, the Netherlands. INPE, 2020. Prodes. Monitoramento do Desmatamento da Floresta Amazonica Brasileira por Satelite.
- Jiménez-Muñoz, J., Mattar, C., Barichivich, J., et al., 2016. Record-breaking warming and extreme drought in the Amazon rainforest during the course of El Niño 2015–2016. Sci. Rep. 6, 33130. https://doi.org/10.1038/srep33130.
- Katsanos, D., Retalis, A., Michaelides, S., 2016. Validation of a high-resolution precipitation database (CHIRPS) over Cyprus for a 30-year period. Atmos. Res. 169, 459–464. https://doi.org/10.1016/j.atmosres.2015.05.015.
- Kendall, M., 1975. Multivariate Analysis. Charles Griffin and Company, London.
- Khanna, J., Medvigy, D., Fueglistaler, S., Walko, R., 2017. Regional dry-season climate changes due to three decades of Amazonian deforestation. Nat. Clim. Chang. 7 (3), 200–204. https://doi.org/10.1038/nclimate3226.
- Lawrence, D., Vandecar, K., 2014. Effects of tropical deforestation on climate and agriculture. Nat. Clim. Chang. 5 (1), 27–36. https://doi.org/10.1038/nclimate2430.
- Leite-Filho, A.T., Soares-Filho, B.S., Davis, J.L., Abrahão, G.M., Börner, J., 2021. Deforestation reduces rainfall and agricultural revenues in the Brazilian Amazon. Nat. Commun. 12 (1), 2591. https://doi.org/10.1038/s41467-021-22840-7.
- Lewis, S.L., Brando, P.M., Phillips, O.L., van der Heijden, G.M.F., Nepstad, D., 2011. The 2010 Amazon drought. Science 331, 554.
- Long, D., Longuevergne, L., Scanlon, B.R., 2014. Uncertainty in evapotranspiration from land surface modeling, remote sensing, and GRACE satellites. Water Resour. Res. 50, 1131–1151. https://doi.org/10.1002/2013WR014581.
- Malhi, Y., Roberts, J.T., Betts, R.A., Killeen, T.J., Li, W., Nobre, C.A., 2008. Climate change, deforestation, and the fate of the Amazon. Science 319, 169–172. https:// doi.org/10.1126/science.1146961.
- MapBiomas Project, 2021. MapBiomas, Collection 6 of Brazilian Land Cover & Use Map Series. Available at. mapbiomas.org. Accessed September 15th, 2021.
- Marengo, J.A., Espinoza, J.C., 2016. Extreme seasonal droughts and floods in Amazonia: causes, trends and impacts. Int. J. Climatol. 36 (3), 1033–1050. https://doi.org/ 10.1002/joc.4420.
- Marengo, J.A., Tomasella, J., Soares, W.R., et al., 2012. Extreme climatic events in the Amazon basin. Theor. Appl. Climatol. 107, 73–85. https://doi.org/10.1007/s00704-011-0465-1
- Marengo, J.A., Tomasella, J., Soares, W., Alves, L.M., Nobre, C.A., 2010. Extreme climatic events in the Amazon basin: climatological and hydrological context of previous floods. Theor. Appl. Climatol. 85, 1–13.
- Marengo, J.A., Tomasella, J., Alves, L.M., Soares, W.R., Rodriguez, D.A., 2011. The drought of 2010 in the context of historical droughts in the Amazon region. Geophys. Res. Lett. 38, L12703. https://doi.org/10.1029/2011GL047436.
- Martens, B., Miralles, D.G., Lievens, H., van der Schalie, R., de Jeu, R.A.M., Fernández-Prieto, D., Beck, H.E., Dorigo, W.A., Verhoest, N.E.C., 2017. GLEAM v3: satellite-based land evaporation and root-zone soil moisture. Geosci. Model Dev. 10, 1903–1925. https://doi.org/10.5194/gmd-10-1903-2017.
- Mu, Y., Biggs, T.W., De Sales, F., 2021a. Forests mitigate drought in an agricultural region of the Brazilian Amazon: atmospheric moisture tracking to identify critical source areas. Geophys. Res. Lett. 48 https://doi.org/10.1029/2020GL091380 e2020GL091380.
- Mu, Y., Biggs, T., Shen, S.S.P., 2021b. Satellite-based precipitation estimates using a dense rain gauge network over the Southwestern Brazilian Amazon: implication for

- identifying trends in dry season rainfall. Atmos. Res. 261, 105741 https://doi.org/10.1016/j.atmosres.2021.105741.
- Nawaz, M., Iqbal, M.F., Mahmood, I., 2021. Validation of CHIRPS satellite-based precipitation dataset over Pakistan. Atmos. Res. 248, 105289.
- Nobre, P., Malagutti, M., Urbano, D.F., de Almeida, R.A.F., Giarolla, E., 2009. Amazon deforestation and climate change in a coupled model simulation. J.Clim. 22, 5686–5697
- Paca, V.H.M., Espinoza-Dávalos, G.E., Moreira, D.M., Comair, G., 2020. Variability of Trends in precipitation across the Amazon River Basin determined from the CHIRPS precipitation product and from station records. Water 12, 1244. https://doi.org/ 10.3390/w12051244.
- Panisset, J.S., Libonati, R., Gouveia, C.M.P., Machado-Silva, F., França, D.A., França, J.R. A., Peres, L.F., 2018. Contrasting patterns of the extreme drought episodes of 2005, 2010 and 2015 in the Amazon Basin. Int. J. Climatol. 38, 1096–1104. https://doi.org/10.1002/joc.5224.
- Paredes-Trejo, F.J., Barbosa, H.A., LakshmiKumar, T.V., 2017. Validating CHIRPS-based satellite precipitation estimates in Northeast Brazil. J. Arid Environ. 139, 26–40. https://doi.org/10.1016/j.jaridenv.2016.12.009.
- Parsons, L.A., 2020. Implications of CMIP6 projected drying trends for 21st century amazonian drought risk. Earth's Future 8 (10). https://doi.org/10.1029/
- Pedreros, D., Tamuka, M., 2020. GeoCLIM Manual 1.2.1. US Geological Survey, Family Early Warning System Network. UC Santa Barbara Climate Hazards Group. https://edcintl.cr.usgs.gov/downloads/sciweb1/shared/fews/geoclim/GeoCLIM 1.2.1 Manual.pdf.
- Ray, D.K., Nair, U.S., Lawton, R.O., Welch, R.M., Pielke, R.A.Sr., 2006. Impact of land use on Costa Rican tropical montane cloud forests: sensitivity of orographic cloud formation to deforestation in the plains. J. Geophys. Res. 111, D02108. https://doi. org/10.1029/2005JD006096.
- Regoto, P., Dereczynski, C., Chou, S.C., Bazzanela, A.C., 2021. Observed changes in air temperature and precipitation extremes over Brazil. Int. J. Climatol. 41 (11), 5125–5142. https://doi.org/10.1002/joc.7119.
- Ronchail, J., Cochonneau, G., Molinier, M., Guyot, J.L., De Miranda Chaves, A.G., Guimarães, V., Oliveira, E., 2002. Interannual rainfall variabil-ity in the Amazon basin and sea-surface temperatures in the equa-torial Pacific and the tropical Atlantic Oceans. Int. J. Climatol. 22, 1663–1686. https://doi.org/10.1002/joc.815
- Santos, E.B., Lucio, P.S., Silva, C.M.S.E., 2015. Precipitation regionalization of the Brazilian Amazon. Atmos. Sci. Lett. 16, 185–192. https://doi.org/10.1002/asl2.535.
- Sen, P.K., 1968. Estimates of regression coefficient based on Kendall's tau. J. Am. Stat. Assoc. 63 (324), 1379–1389. https://doi.org/10.1080/01621459.1968.10480934. Siegel, A.F., 1982. Robust regression using repeated medians. Biometrika 69 (1),
- Siegel, A.F., 1982. Robust regression using repeated medians. Biometrika 69 (1), 242–244.
- Silva Junior, C.H.L., Almeida, C.T., Santos, J.R.N., Anderson, L.O., Aragão, L.E.O.C., Silva, F.B., 2018. Spatiotemporal rainfall trends in the Brazilian legal amazon between the years 1998 and 2015. Water 10, 1220. https://doi.org/10.3390/w10091220.
- Sörensson, A.A., Ruscica, R.C., 2018. Intercomparison and uncertainty assessment of nine evapotranspiration estimates over South America. Water Resour. Res. 54, 2891–2908. https://doi.org/10.1002/2017WR021682.
- Souza Jr., C.M., Siqueira, J.V., Sales, M.H., Fonseca, A.V., Ribeiro, J.G., Numata, I., Cochrane, M.A., Barber, C.P., Roberts, D.A., Barlow, J., 2013. Ten-Year Landsat classification of deforestation and forest degradation in the Brazilian Amazon. Remote Sens. 5 (11), 5493–5513. https://doi.org/10.3390/rs5115493.
- Souza Jr., Carlos M., Shimbo, Julia Z., Rosa, Marcos R., Parente, Leandro L., Alencar, Ane A., Bernardo, F.T., et al., 2020. Reconstructing three decades of land use and land cover changes in Brazilian Biomes with Landsat archive and earth engine. Remote Sens. 12 (17), 2735. https://doi.org/10.3390/rs12172735.
- Staal, A., Tuinenburg, O.A., Bosmans, J.H.C., Holmgren, M., van Nes, E.H., Scheffer, M., et al., 2018. Forest-rainfall cascades buffer against drought across the Amazon. Nat. Clim. Chang. 8 (6), 539–543. https://doi.org/10.1038/s41558-018-0177-y.
- Staal, A., Flores, B.M., Aguiar, A.P.D., Bosmans, J.H., Fetzer, I., Tuinenburg, O.A., 2020. Feedback between drought and deforestationin the Amazon. Environ. Res. Lett. 15 (4), 044024.
- Theil, H., 1992. A rank-invariant method of linear and polynomial regression analysis. In: Raj, B., Koerts, J. (Eds.), Henri Theil's Contributions to Economics and Econometrics. Advanced Studies in Theoretical and Applied Econometrics, vol 23. Springer, Dordrecht. https://doi.org/10.1007/978-94-011-2546-8_20.
- Tian, Y., Peters-Lidard, C.D., 2010. A global map of uncertainties in satellite-based precipitation measurements. Geophys. Res. Lett. 37, L24407. https://doi.org/ 10.1029/2010GL046008.
- van der Ent, R.J., Savenije, H.H.G., Schaefli, B., Steele-Dunne, S.C., 2010. Origin and fate of atmospheric moisture over continents. Water Resour. Res. 46, W09525. https:// doi.org/10.1029/2010WR009127.
- Wongchuig, S., Espinoza, J.C., Condom, T., Segura, H., Ronchail, J., Arias, P.A., Junquas, C., Rabatel, A., Lebel, T., 2021. A regional view of the linkages between hydro-climatic changes and deforestation in the Southern Amazon. Int. J. Climatol. 1–19. https://doi.org/10.1002/joc.7443.
- Wu, Y., Guo, L., Zheng, H., Zhang, B., Li, M., 2019. Hydroclimate assessment of gridded precipitation products for the Tibetan Plateau. Sci. Total Environ. 660, 1555–1564. https://doi.org/10.1016/j.scitotenv.2019.01.119.
- Zilli, M.T., Carvalho, L.M.V., Liebmann, B., Silva, M.A., 2017. A comprehensive analysis of trends in extreme precipitation over southeastern coast of Brazil. Int. J. Climatol. 37, 2269–2279. https://doi.org/10.1002/joc.4840.